Check for updates

High Power Laser Science and Engineering, (2026), Vol. 14, e48, 7 pages.
doi:10.1017/hpl.2026.10140

HIGH POWER LASER SCIENCE AND ENGINEERING

LETTER

Preservation of ^{3}He ion polarization after laser-driven acceleration in plasma

Chuan Zheng[1,2,3,4], Pavel Fedorets[1], Zahra Marjan Chitgar[5], Ralf Engels[6], Ilhan Engin[7], Paul Gibbon[5], Harald Glückler[8], Chrysovalantis Kannis[2], Alexander Pukhov[9], Lars Reichwein[1,9], Norbert Schnitzler[1], Helmut Soltner[8], Bernhard Zielbauer[10], and Markus Büscher[1,2]

[1] *Peter Grünberg Institute, Forschungszentrum Jülich GmbH, Jülich, Germany*

[2] *Institute for Laser and Plasma Physics, Heinrich Heine University Düsseldorf, Düsseldorf, Germany*

[3] *ExtreMe Matter Institute EMMI, GSI Helmholtzzentrum für Schwerionenforschung, Darmstadt, Germany*

[4] *Artemis Targetra GmbH, Aachen, Germany*

[5] *Jülich Supercomputing Centre, Forschungszentrum Jülich GmbH, Jülich, Germany*

[6] *Nuclear Physics Institute, Forschungszentrum Jülich GmbH, Jülich, Germany / GSI Helmhotzzentrum für Schwerionenforschung, Darmstadt, Germany*

[7] *Stabsstelle Arbeitssicherheit, Forschungszentrum Jülich GmbH, Jülich, Germany*

[8] *Institute of Technology and Engineering, Forschungszentrum Jülich GmbH, Jülich, Germany*

[9] *Institute for Theoretical Physics I, Heinrich Heine University Düsseldorf, Düsseldorf, Germany*

[10] *Plasma Physics Department, GSI Helmholtzzentrum für Schwerionenforschung, Darmstadt, Germany*

(Received 19 January 2026; revised 13 March 2026; accepted 10 April 2026)

Abstract

The preservation of nuclear spin alignment in plasmas is a prerequisite for important applications, such as energy production through polarized fusion or the acceleration of polarized particle beams. Although this conservation property has been the basis of numerous theoretical papers, it has never been experimentally confirmed. Here, we report on first experimental data from a polarized ^{3}He target heated by a PW laser pulse, showing evidence consistent with the persistence of nuclear polarization after acceleration to MeV energies via Coulomb explosion of a plasma channel. Our results confirm the theoretically established concept of using pre-polarized targets for experiments in high-power laser facilities.

Keywords: high-power laser; laser–plasma acceleration; polarimetry; polarized beams

1. Introduction

Spin dynamics in plasmas is a flourishing field of research that studies how the spin of particles such as electrons, ions and positrons evolves in plasma environments, especially under high-energy conditions such as in plasma accelerators or fusion reactors. Key aspects of spin dynamics include generating spin polarization, understanding spin precession and the effects of intense electromagnetic fields in plasma environments. All potential applications critically depend on the ability to maintain the spin alignment of particles (i.e., their polarization) in the plasma for a sufficiently long period of time compared to the typical timescales involved[1].

The worldwide strategic processes[2–4] aiming at the realization of next-generation particle accelerators point at the importance of polarized beams (leptons, protons and ions) for fundamental research and various applications. Dozens of theoretical papers have been published in recent years on the feasibility of polarized beam generation in plasma accelerators (see, e.g., the review paper by Reichwein *et al.*[5] for an overview).

Almost a century ago, Goldhaber[6] inferred that fusion cross-sections depend on the relative spin orientation of the participating nuclei (i.e., the 'fuel'). Typical enhancement factors, for example for the total $d+t \rightarrow \alpha + n$ cross-section, amount to roughly 50%[7,8]. In their seminal 1982 paper[9], Kulsrud *et al.* predicted time scales for polarization loss

Correspondence to: M. Büscher, Peter Grünberg Institute, Forschungszentrum Jülich GmbH, 52425 Jülich, Germany. Email: m.buescher@fz-juelich.de

© The Author(s), 2026. Published by Cambridge University Press in association with Chinese Laser Press. This is an Open Access article, distributed under the terms of the Creative Commons Attribution licence (https://creativecommons.org/licenses/by/4.0), which permits unrestricted re-use, distribution and reproduction, provided the original article is properly cited.

https://doi.org/10.1017/hpl.2026.10140 Published online by Cambridge University Press

in the plasma of a magnetic fusion reactor to be much longer than the characteristic fuel burn-up period. A research project to measure the lifetime of spin-polarized fuel at the DIII-D reactor in San Diego is finally under way[8,10]. Further advantages of polarized fusion are facilitated neutron management and an increased tritium burn efficiency that may significantly reduce the startup tritium inventory[11]. Note that all of these advantages should also apply to inertial fusion[12]; a more comprehensive discussion can be found in Refs. [7,13].

The typical association of nuclear spin alignment is with low temperatures, making it counter-intuitive that it could endure in a 10^8 Kelvin plasma long enough to have practical applications. On the other hand, a theoretical study[1] of the scaling laws for depolarization times indicated the feasibility of polarized particle acceleration in strong plasma fields. Experimental tests on the polarization conservation are challenging[8,10,14,15] and have not been carried out up to now.

Here, we report the findings of an experimental campaign using a nuclear-spin-polarized ^{3}He gas jet as the target[16] for a petawatt laser pulse. ^{3}He – the isospin partner of ^{3}H – has the advantages that it is not radioactive, can be polarized at room temperature and can be stored over a long time in moderate (mT) magnetic holding fields. Laser-generated ^{3}He plasmas, heated to the fusion resonance energies, are therefore an ideal testbed for polarized fusion. We present the first experimental evidence that the initial nuclear polarization is essentially preserved during the laser-induced heating and ionization and the subsequent acceleration of the ions from the plasma to MeV energies. Our data also point to the need for further scattering experiments with polarized ^{3}He beams or targets, as the absolute polarization values of the accelerated ^{3}He ions could not be determined due to insufficient quality of analysing-power data in literature.

2. Experimental setup

2.1. Polarized target

The laser pulses were provided by the PHELIX petawatt laser at GSI Darmstadt[17] and contained about 50 J energy each. The optimal pulse duration of 2.2 ps for the acceleration of $^3He^{1+,2+}$ ions had been found during a previous measurement with unpolarized gas[18]. The polarizer[19] for the ^{3}He gas was operated at Forschungszentrum Jülich, located roughly 250 km from GSI. Unfortunately, due to small amounts of oxygen leaking into the polarizer, the initial gas polarization did not exceed approximately 50%, as opposed to values of 75% that were achieved during the preparatory phase[16]. Due to various depolarization mechanisms, the initial gas polarization decreases exponentially in time. The polarized gas was stored in transport cells made of a special glass at an initial gas pressure of 3 bar; a glass ball with

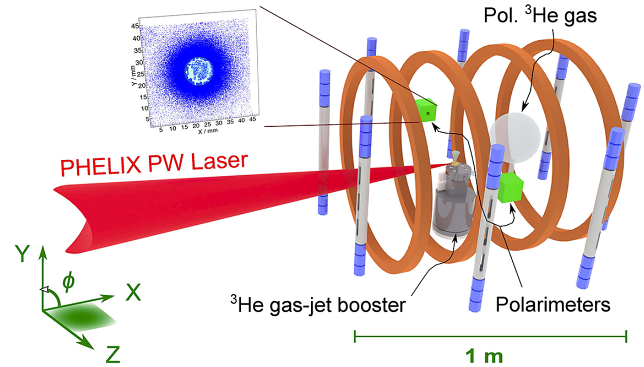

Figure 1. Experimental setup at PHELIX: the laser beam (red) hits the polarized ^{3}He gas jet that is emitted in the $+Y$ direction. The magnetic system comprises a permanent magnet arrangement with eight vertical pillars (horizontal field in the $+Z$ direction) and a Helmholtz-coil array for spin-orientation manipulation in the X–Z plane. Two polarimeters (green), located inside radiation-protecting boxes (not shown), are mounted at right angles relative to the laser propagation axis X with a direct view on the laser–plasma interaction region. The insert shows data from a front detector plate in one polarimeter on elastically scattered ^{3}He ions.

fresh gas was re-supplied to the PHELIX target chamber (cf. Figure 1) every morning. With the help of a non-magnetic gas compressor this pressure can be enhanced before each laser shot to a maximum value of 30 bar. The jet of 1 mm diameter is formed with the help of a titanium de Laval nozzle mounted on a non-magnetic valve, both located on top of the pressure booster. This leads to super-Gaussian distributed jet densities of a few times 10^{19} cm^{-3} which are required for the acceleration of the ^{3}He ions to MeV energies[18]. During the gas compression and jet formation the final ^{3}He polarization decreased to half of the initial value[16].

The initial ^{3}He polarization along $+Z$ is maintained by a permanent magnetic holding field of 1.3 mT[20]. Then the polarization ($P_Z/P = 1$) is (anti-)parallel to the momentum vector of the ejected ions (pointing at the two polarimeters) – this is the case of longitudinal polarization, which is undetectable in the polarimeters. Additional Helmholtz coils (maximum current 10 A, corresponding to 5 mT)[16,20] allow one to rotate the initial ^{3}He polarization in the horizontal plane towards $+X$ or $-X$ to achieve the transverse polarization case (maximum $P_X/P = \pm 0.97$). Such a polarization is measurable since it can induce a top–bottom (Y direction) rate asymmetry in scattering data of the polarimeters; cf. Figure 2.

2.2. Polarimetry

Two identical polarimeters[22] are used to measure the remaining polarization of the accelerated ^{3}He ions. They are placed at right angles relative to the laser propagation axis X at distances of 95 mm (at $+Z$, see Figure 1) and 264 mm ($-Z$), respectively. The angular acceptances of the two polarimeters differ by a factor approximately eight –

https://doi.org/10.1017/hpl.2026.10140 Published online by Cambridge University Press

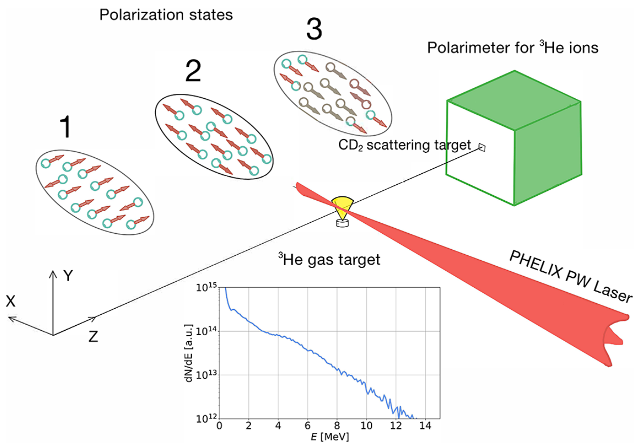

Figure 2. Principle of the polarization manipulation and measurement with the polarized ^{3}He target. Depending on the currents in the Helmholtz coils, the ^{3}He gas can initially be longitudinally (case 1, zero current) or transversally (cases 2 and 3) polarized. The inserted spectrum is an approximation of the measured[18] ^{3}He energy distribution by a PIC simulation[21].

below we present data for the near polarimeter; the results for its far counterpart support our findings but exhibit lower statistical accuracy. Each cube-shaped polarimeter contains a collimator (defining a 3 mm diameter beam), a CD_2 foil target for secondary scattering of the ions and five CR-39 detector plates (front, left, right, top, bottom) for particle identification. Two types of reactions in the foil target are used for the analysis, that is, (elastic) Rutherford scattering of the accelerated ^{3}He ions and the ^{2}H($^3\overrightarrow{\mathrm{H}}$e, ^{4}He)^{1}H fusion reaction that transforms the ^{3}He polarization information into a measurable azimuthal angular (ϕ as defined in Figure 1) asymmetry of the emitted α particles via a non-vanishing analysing power A; see Ref. [22] for details.

The Rutherford-scattering data (cf. Figure 1) are dominated by few-MeV ^{3}He ions[18] deflected by the carbon atoms of the foil, which has a total thickness of approximately 10 μm (6 μm CD_2 + 4 μm CH_2). It is not sensitive to beam polarization ($A = 0$); however, it can reveal asymmetries of the beam profile in the transverse phase space (X/X' and Y/Y'), which are caused by the plasma acceleration and space-charge effects. The fusion reaction is much less sensitive to the transverse beam profile due to its large Q value (18.35 MeV) and the small observed effects can be explained by the Rutherford-scattering data. The field of the Helmholtz coils causes a very small deflection of the ^{3}He ions on their way to the polarimeter ($\sim 0.2°$ for 2 MeV ions) and does not affect the transverse beam profile.

3. Data analysis

We present the results of four days of data acquisition; during each day we recorded five to six laser shots for three different orientations of the ^{3}He polarization and one for the control measurement with unpolarized ^{3}He gas. We focus on a comparison of two data sets for the Helmholtz coils switched on but in the opposite direction (transverse polarization, cases 2 and 3 in Figure 2), with emphasis on the azimuthal angular asymmetries of the α particles from the ^{2}H($^3\overrightarrow{\mathrm{H}}$e, ^{4}He)^{1}H reaction. The flux of ^{3}He ions emitted into the direction of the near polarimeter can be estimated from the number of detected α particles as 2.0×10^{12} particles/sr per shot, while the average number of ^{3}He ions above the fusion-reaction threshold hitting the CD_2 foil target is roughly 1.6×10^9 particles per shot.

The angular distribution of the count-rate difference $\varepsilon(\phi) = \left(N_{\mathrm{top}}(\phi) - N_{\mathrm{bottom}}(\phi + 180°)\right) / \left(N_{\mathrm{top}}(\phi) + N_{\mathrm{bottom}}(\phi + 180°)\right)$, deduced individually in four separate detector regions, is depicted in Figure 3. We use the rate differences since they are less affected by systematic uncertainties such as background suppression and detector efficiencies. The data points outside the 50°–130° angular range could not be extracted from the left- and right-hand plates since the signal tracks on these plates were not sufficiently well formed during the etching procedure.

The ^{3}He polarization P is related to $\varepsilon(\phi)$ according to the following formula:

$$P = \frac{\varepsilon(\phi)}{A(E,\theta) \cdot \sin(\phi - \phi_{\mathrm{P}})}, \qquad (1)$$

where $A(E,\theta)$ is the analysing power, which depends on the ^{3}He energy E and the polar angle θ of the detected α particles (40°–80°[22]), and ϕ_{P} is the azimuthal polarization angle. In our case a precise determination of P from the measured $\varepsilon(\phi)$ is not possible since it would require the knowledge of A in the full (E,θ) space of our measurement (cf. insert in Figure 2 for the ^{3}He energy distribution) as well as the exact energy distribution of the ^{3}He ions undergoing the fusion reaction after deceleration in the CD_2 foil.

For the transverse cases a count-rate asymmetry must change sign for a reversal of the Helmholtz field orientation[14,22]. This is, of course, only true under the assumption that the ^{3}He ions are still transversely polarized after acceleration. Figure 3 shows that the measured angular distributions $\varepsilon(\phi)$ exactly reveal this ‘spin-flip’ behaviour. In the absence of a polarization persistence, the green and pink data points would be centred around $\varepsilon(\phi) = 0$ as indicated by the blue line. Figure 3 also shows fits of functions $\varepsilon(\phi) = \varepsilon_0 \sin(\phi - \phi_0)$ to the two data sets. The best fits result in values of $\varepsilon_0 = 0.15 \pm 0.03$ and 0.12 ± 0.03, respectively, that is, a statistical significance of more than 5σ.

In contrast to the two data sets for transverse polarization, one does not expect an asymmetry for unpolarized ^{3}He gas, which is precisely what was observed for the integrated top–bottom count-rate difference $\varepsilon = (N_{\mathrm{t}} - N_{\mathrm{b}}) / (N_{\mathrm{t}} + N_{\mathrm{b}}) =$

https://doi.org/10.1017/hpl.2026.10140 Published online by Cambridge University Press

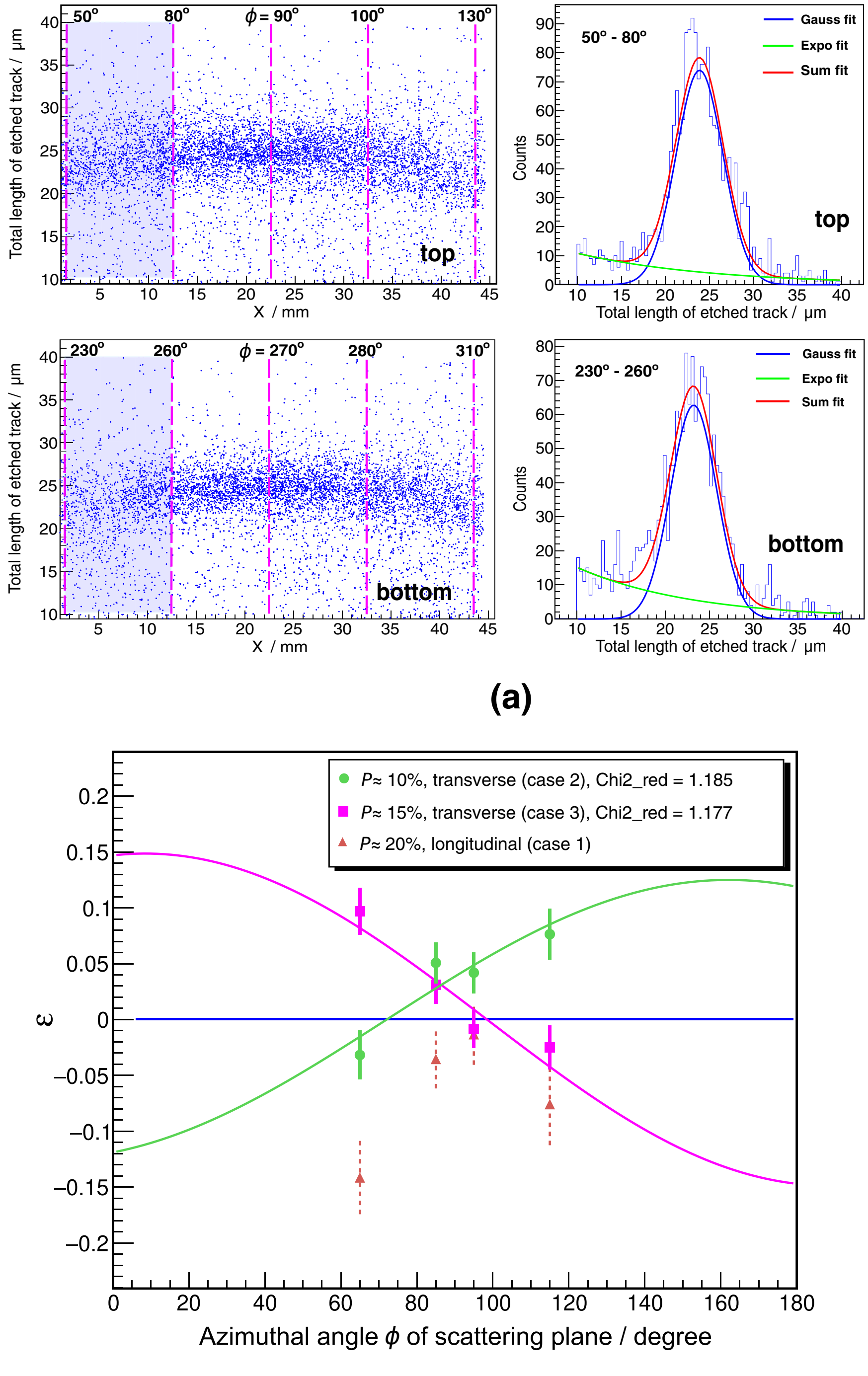

Figure 3. (a) Hit pattern of the α particles on the top and bottom plates (left) for one field direction. Extraction of the fusion events by fitting a Gaussian function to the signal and an exponential function to the background (right). This procedure is applied in four angular bins in the ϕ range of 50°–130° (top detector) and on the opposite side. (b) Count-rate difference ε of the α particles derived from the procedure described in (a). The error bar of each point is calculated from the total number of events under the signal peak including the background within a '3σ region' of the Gaussian function. The green and pink lines are linear fits to the data to provide visual guidance. The initial degree[22] and orientation of the polarization in the jet are indicated.

-0.010 ± 0.016. An irregular shape, limited to a small ϕ-angle range, is observed in the corresponding Rutherford-scattering data on the front plate, and explains a count-rate fluctuation on the left-hand plate. As can be seen from Figure 3, the quality of the data for longitudinal polarization (case 1 in Figure 2) is very poor as the $\varepsilon(\phi)$ distribution exhibits large statistical fluctuations and cannot be reasonably described by a sinosoidal fit function (χ^2_{black} values larger than 4). We have therefore excluded these data from a detailed statistical analysis.

https://doi.org/10.1017/hpl.2026.10140 Published online by Cambridge University Press

4. Discussion

4.1. GEANT4 simulations

In principle, the asymmetry observed in the distributions of $\varepsilon(\phi)$ for cases of transverse polarization could be caused by rate fluctuations over the cross-section of the ^{3}He ion beams entering the polarimeter. In order to estimate the relevance of such effects we have carried out simulations with the GEANT4 and G4BEAMLINE codes. These simulations were performed under the assumption that circular 3 mm diameter beams of 10^9 $^3He^{2+}$ ions enter the polarimeter and the beam profiles vary up to the unrealistic case (since the observed Rutherford-scattering distributions exhibit only small fluctuations in the beam profiles) where all ions are contained within one semicircle of the beam profile. It turns out that the count-rate asymmetries $\varepsilon(\phi)$ can be explained to only a small extent by irregularly shaped transverse phase spaces (and mimic a higher polarization value) since space-charge effects in the $^3He^{2+}$ bunches tend to dilute the angular asymmetries.

4.2. Particle-in-cell simulations

In order to assess the efficiency of the ^{3}He ion acceleration and preservation of spin polarization, we have conducted two-dimensional (2D) particle-in-cell (PIC) simulations[21] with the EPOCH[23] and the VLPL codes[24,25]. To match the experimental parameters, a laser intensity of 1.38×10^{19} W cm^{-2} with 1.053 μm wavelength and a pulse duration of 0.8 ps (full width at half maximum, FWHM) was taken, focused down to a spot size of 25.7 μm (FWHM) in the centre of a round, 1 mm diameter ^{3}He gas-jet target with a sixth-order super-Gaussian density profile at 4.75×10^{19} cm^{-3}. The computational grid covered 2.0 mm × 2.0 mm with resolution of 0.04 μm in each dimension and roughly 1.5 particles per cell.

The codes include a module for the Thomas–Bargmann–Michel–Telegdi (T-BMT) equation[26] describing spin precession. The assumed initial spin direction is that of laser propagation, that is, $s_X=\hbar/2$. When the laser pulse irradiates the ^{3}He target, its ponderomotive force expels the electrons mainly towards the front and at right angles to laser propagation, leaving behind a plasma channel with a strong magnetic field (few 10^3 T). The charge separation then induces a Coulomb explosion, leading to the acceleration of the ^{3}He ions at a ±90° angle. The same acceleration mechanism was identified in the study of the unpolarized ^{3}He and ^{4}He targets[18]. At the falling edge of the gas jet, a displacement between the electronic and ionic plasma components leads to an acceleration process in the forward direction similar to target normal sheath acceleration[27,28]. These forward accelerated ions, however, make up only a small part of the total number of accelerated ^{3}He ions for our laser-target configuration. If shorter targets were utilized, more ions in the forward direction would be expected[21]. Both simulation codes show that the ions gain only small s_Y, s_Z components in their spin vector due to a precession around the strong magnetic field of the plasma channel that is fully compatible with the observed polarization conservation.

4.3. Analytical estimates

In simplified terms, the $^3He^{2+}$ ions perform two types of motion in the magnetic field of the plasma: the cyclotron motion and the precession of the nuclear magnetic moment $\vec{\mu}_i$. This can be described by two non-relativistic equations as follows:

$$\frac{d\vec{v}_i}{dt}=\frac{q_i}{m_i}\left(\vec{v}_i\times\vec{B}\right), \tag{2}$$

$$\frac{d\vec{\mu}_i}{dt}=\gamma_h\left(\vec{\mu}_i\times\vec{B}\right), \tag{3}$$

where $\vec{v}_i$, q_i and m_i are ion velocity, charge and mass, respectively, and γ_h is the gyromagnetic ratio of ^{3}He nuclei, $\vec{\mu}=\gamma_h\vec{s}$. The magnetic moment $\vec{\mu}$ is antiparallel to the nuclear spin $\vec{s}$, which is expressed by a minus sign of γ_h.

We assume a simple model of the magnetic field $\vec{B}$ around the 1 mm long plasma channel induced by the laser pulse with a focus spot of 10 μm × 10 μm. The electrons are pushed forward along the channel, corresponding to an electric current I_e (tens of kA) opposite to the direction of laser propagation, and according to Biot–Savart's law a vortex magnetic field $B_\varphi(r)=\mu_0 I_e/(2\pi r)$ builds up around the channel. This field then rotates the velocity vectors $\vec{v}_i$ and the spin directions $\vec{\mu}_i$ in the horizontal plane according to Equations (2) and (3). The rotational effect on $\vec{v}_i$ was measured in our previous experiment at ±90° for ^{4}He ions[18] and leads to a backward bending of 2°, which is also confirmed by the PIC simulations.

Since the cyclotron motion and the spin precession are caused by the same local magnetic field $\vec{B}$, the rotational effect on the magnetic moment $\vec{\mu}_i$ along a ^{3}He ion trajectory can be deduced from the cyclotron and the precession frequencies of the $^3He^{2+}$ ions:

$$\omega_c=\frac{q_i B}{m_i}=0.641\times10^8 B\,[\mathrm{T}]\ \mathrm{rad/s}, \tag{4}$$

$$\omega_s=\gamma_h B=-2.038\times10^8 B\,[\mathrm{T}]\ \mathrm{rad/s}, \tag{5}$$

which have a fixed ratio of $\omega_s/\omega_c=-3.18$. The backward bending angle $\Delta\theta_c=\int q_i/m_i B_y(x,z,t)\,dt$ is estimated as 2.7° for ^{3}He ions. Then the precession angle $\Delta\theta_s=\int\gamma_h B_y(x,z,t)\,dt$ is expected to be 8.5° opposite to that of the cyclotron motion. This corresponds to a small

https://doi.org/10.1017/hpl.2026.10140 Published online by Cambridge University Press

change of the X-component of the initial polarization from $P_X/P = 1$ to 0.99, which is consistent with the simulation result[21].

5. Conclusions and outlook

We present results of a first experiment using a polarized target at a high-power laser facility and demonstrate their feasibility for the acceleration of polarized particles. Most notably we observe an angular asymmetry of the α particles in our polarimeter, which we can only explain by a transverse polarization of the accelerated ^{3}He ions. It is therefore shown that the transverse polarization of the nuclear spins is at least partially conserved (according to PIC simulations to more than 99%) during plasma heating and acceleration to MeV energies. This is a first hint that nuclear polarization survives a laser-induced plasma and, therefore, the advantages of polarized fuel are useable for this type of fusion reactor.

An absolute polarization measurement of the ^{3}He ions is not feasible because the values of the ^{2}H($^3\overrightarrow{\mathrm{H}}$e, ^{4}He)^{1}H analysing power are not known for the full energy range of the accelerated ^{3}He ions, and the energy distributions of the ^{3}He ions reaching the polarimeters are not precisely known. Our measurements were also limited by the low ($\lesssim$ 20% in the jet) initial polarization of the target gas due to vacuum leaks in our ^{3}He polarizer. We note that our conclusions are based on relative measurements (such as the change of sign of angular asymmetries in Figure 3(b)) and are averaged over five or six laser shots, making them robust to fluctuations of the laser intensity or target density, and plasma filamentation[18].

It is planned to continue the experiments at PHELIX at higher gas polarization, and using a narrower (0.5 mm instead of 1.0 mm) gas-jet target. This would have the advantage that the ^{3}He ions should be dominantly emitted under 0° and at significantly higher energies (10–15 MeV)[21]. In parallel we developed a polarized HCl gas target[29] for laser- or beam-driven acceleration of polarized proton and electron beams[30–36]. This target could also be operated with deuterium iodide (DI) gas[37] and be combined with polarized ^{3}He in order to further study options for polarized fusion with high-power lasers.

Acknowledgements

This work has been carried out in the framework of the JuSPARC (Jülich Short-Pulse Particle and Radiation Center) project[38] and has been supported by the ATHENA consortium (Accelerator Technology HElmholtz iNfrAstructure) in the ARD programme (Accelerator Research and Development) of the Helmholtz Association. We acknowledge funding through the European Union's Horizon Europe research and innovation programme under grant agreement No. 101079773 (EuPRAXIA Preparatory Phase Project). Our results are based on experiment P191, which was performed at the PHELIX infrastructure at GSI Helmholtzzentrum für Schwerionenforschung, Darmstadt (Germany) in the context of FAIR Phase-0. The authors gratefully acknowledge the Gauss Centre for Supercomputing e.V.[39] for funding this project by providing computing time through the John von Neumann Institute for Computing (NIC) on the GCS Supercomputer JUWELS at Jülich Supercomputing Centre (JSC). MB acknowledges support by the CAS President's International Fellowship Initiative. Special thanks go to Werner Heil (retired Professor from Johannes Gutenberg-University Mainz) for providing the ^{3}He polarizer and for answering many emergency calls.

References

1. J. Thomas, A. Hützen, A. Lehrach, A. Pukhov, L. Ji, Y. Wu, X. Geng, and M. Büscher, Phys. Rev. Accel. Beams **23**, 064401 (2020).
2. N. Mounet, *European Strategy for Particle Physics - Accelerator R&D Roadmap*, CERN Yellow Reports: Monographs, CERN-2022-001 (CERN, Geneva, 2022).
3. M. Fuchs, B. A. Shadwick, N. Vafaei-Najafabadi, A. G. R. Thomas, G. Andonian, M. Büscher, A. Lehrach, O. Apsimon, G. Xia, D. Filippetto, C. B. Schroeder, and M. C. Downer, arXiv:2203.08379 (2022).
4. D. P. Anderle, V. Bertone, X. Cao, L. Chang, *et al.*, Front. Phys. **16**, 64701 (2021).
5. L. Reichwein, Z. Gong, C. Zheng, L. L. Ji, A. Pukhov, and M. Büscher, Rep. Prog. Phys. **88**, 117001 (2025).
6. M. Goldhaber, Math. Proc. Camb. Philos. Soc. **30**, 561 (1934).
7. H. Paetz gen. Schieck, Eur. Phys. J. A **44**, 321 (2010).
8. L. R. Baylor, A. Deur, N. W. Eidietis, W. W. Heidbrink, G. L. Jackson, J. Liu, M. M. Lowry, G. W. Miller, D. C. Pace, A. M. Sandorfi, S. P. Smith, S. Tafti, K. Wei, X. Wei, and X. Zheng, Nucl. Fusion **63**, 076009 (2023).
9. R. M. Kulsrud, H. P. Furth, E. J. Valeo, and M. Goldhaber, Phys. Rev. Lett. **49**, 1248 (1982).
10. W. W. Heidbrink, L. R. Baylor, M. Büscher, R. W. Engels, A. V. Garcia, A. G. Ghiozzi, G. W. Miller, A. M. Sandorfi, X. Wei, and X. Zheng, Front. Phys. **12**, 1355212 (2024).
11. J. F. Parisi, A. Diallo, and J. A. Schwartz, Nucl. Fusion **64**, 126019 (2024).
12. M. Temporal, V. Brandon, B. Canaud, J. P. Didelez, R. Fedosejevs, and R. Ramis, Nucl. Fusion **52**, 103011 (2012).
13. G. Ciullo, R. Engels, M. Büscher, and A. Vasilyev, *Nuclear Fusion with Polarized Fuel* (Springer International Publishing, Cham, 2016).
14. N. Raab, M. Büscher, M. Cerchez, R. Engels, I. Engin, P. Gibbon, P. Greven, A. Holler, A. Karmakar, A. Lehrach, R. Maier, M. Swantusch, M. Toncian, T. Toncian, and O. Willi, Phys. Plasmas **21**, 023104 (2014).
15. M. Büscher, A. Hützen, L. Ji, and A. Lehrach, High Power Laser Sci. Eng. **8**, e36 (2020).
16. P. Fedorets, C. Zheng, R. Engels, I. Engin, H. Feilbach, U. Giesen, H. Glückler, C. Kannis, F. Klehr, M. Lennartz, H. Pfeifer, J. Pfennings, C. M. Schneider, N. Schnitzler, H. Soltner, R. Swaczyna, and M. Büscher, Instruments **6**, 18 (2022).
17. V. Bagnoud, B. Aurand, A. Blazevic, S. Borneis, C. Bruske, B. Ecker, U. Eisenbarth, J. Fils, A. Frank, E. Gaul, S. Goette,

https://doi.org/10.1017/hpl.2026.10140 Published online by Cambridge University Press

C. Haefner, T. Hahn, K. Harres, H.-M. Heuck, D. Hochhaus, D. H. H. Hoffmann, D. Javorková, H.-J. Kluge, T. Kuehl, S. Kunzer, M. Kreutz, T. Merz-Mantwill, P. Neumayer, E. Onkels, D. Reemts, O. Rosmej, M. Roth, T. Stoehlker, A. Tauschwitz, B. Zielbauer, D. Zimmer, and K. Witte, Appl. Phys. B **100**, 137 (2010).
18. I. Engin, Z. M. Chitgar, O. Deppert, L. Di Lucchio, R. Engels, P. Fedorets, S. Frydrych, P. Gibbon, A. Kleinschmidt, A. Lehrach, R. Maier, D. Prasuhn, M. Roth, F. Schlüter, C. M. Schneider, T. Stöhlker, K. Strathmann, and M. Büscher, Plasma Phys. Controlled Fusion **61**, 115012 (2019).
19. C. Mrozik, O. Endner, C. Hauke, W. Heil, S. Karpuk, J. Klemmer, and E. W. Otten, J. Phys. Conf. Ser. **294**, 012007 (2011).
20. H. Soltner, M. Büscher, P. Burgmer, I. Engin, B. Nauschütt, S. Maier, and H. Glückler, IEEE Trans. Appl. Supercond. **26**, 0603704 (2016).
21. P. Gibbon, Z. Chitgar, M. Büscher, P. Fedorets, A. Lehrach, X. Li, and C. Zheng, in *48th EPS Conference on Plasma Physics* (2022).
22. C. Zheng, P. Fedorets, R. Engels, C. Kannis, I. Engin, S. Möller, R. Swaczyna, H. Feilbach, H. Glückler, M. Lennartz, H. Pfeifer, J. Pfennings, C. M. Schneider, N. Schnitzler, H. Soltner, and M. Büscher, Instruments **6**, 61 (2022).
23. T. D. Arber, K. Bennett, C. S. Brady, A. Lawrence-Douglas, M. G. Ramsay, N. J. Sircombe, P. Gillies, R. G. Evans, H. Schmitz, A. R. Bell, and C. P. Ridgers, Plasma Phys. Controlled Fusion **57**, 113001 (2015).
24. A. Pukhov, J. Plasma Phys. **61**, 425 (1999).
25. A. Pukhov, arXiv:1510.01071 (2015).
26. V. Bargmann, L. Michel, and V. L. Telegdi, Phys. Rev. Lett. **2**, 435 (1959).
27. L. Willingale, S. P. D. Mangles, P. M. Nilson, R. J. Clarke, A. E. Dangor, M. C. Kaluza, S. Karsch, K. L. Lancaster, W. B. Mori, Z. Najmudin, J. Schreiber, A. G. R. Thomas, M. S. Wei, and K. Krushelnick, Phys. Rev. Lett. **96**, 245002 (2006).
28. A. Lifschitz, F. Sylla, S. Kahaly, A. Flacco, M. Veltcheva, G. Sanchez-Arriaga, E. Lefebvre, and V. Malka, New J. Phys. **16**, 033031 (2014).
29. A. Hützen, J. Thomas, J. Böker, R. Engels, R. Gebel, A. Lehrach, T. P. R. Alexander Pukhov, D. Sofikitis, and M. Büscher, High Power Laser Sci. Eng. **7**, e16 (2019).
30. M. Wen, M. Tamburini, and C. H. Keitel, Phys. Rev. Lett. **122**, 214801 (2019).
31. Y. Wu, L. Ji, X. Geng, Q. Yu, N. Wang, B. Feng, Z. Guo, W. Wang, C. Qin, X. Yan, L. Zhang, J. Thomas, A. Hützen, T. P. R. Markus Büscher, A. Pukhov, B. Shen, and R. Li, New J. Phys. **21**, 073052 (2019).
32. Y. Wu, L. Ji, X. Geng, J. Thomas, M. Büscher, A. Pukhov, A. Hützen, L. Zhang, B. Shen, and R. Li, Phys. Rev. Appl. **13**, 044064 (2020).
33. L. Jin, M. Wen, X. Zhang, A. Hützen, J. Thomas, M. Büscher, and B. Shen, Phys. Rev. E **102**, 011201 (2020).
34. H. C. Fan, X. Y. Liu, X. F. Li, J. F. Qu, Q. Yu, Q. Kong, S. M. Weng, M. Chen, M. Büscher, P. Gibbon, S. Kawata, and Z. M. Sheng, New J. Phys. **24**, 083047 (2022).
35. X. Yan, Y. Wu, X. Geng, H. Zhang, B. Shen, and L. Ji, Phys. Plasmas **29**, 053101 (2022).
36. L. Reichwein, A. Pukhov, and M. Büscher, Phys. Rev. Accel. Beams **25**, 081001 (2022).
37. D. Sofikitis, C. S. Kannis, G. K. Boulogiannis, and T. P. Rakitzis, Phys. Rev. Lett. **121**, 083001 (2018).
38. F. Jülich, J. Large Scale Res. Facil. **6**, A138 (2020).
39. https://www.gauss-centre.eu.

https://doi.org/10.1017/hpl.2026.10140 Published online by Cambridge University Press